ICMIEE22-054

Numerical Investigation of the Aerodynamic Characteristics of a Train Passing through a Tunnel

Koushik Ahmed[1,*], *Mohammad Ilias Inam*[1]
[1] Department of Mechanical Engineering, Khulna University of Engineering & Technology, Khulna-9203, BANGLADESH

ABSTRACT
The limitation of geographical space has been a major concern in Bangladesh. So, tunneling may be a solution for the demand of quality and efficient transport with the increasing population. Hence, it is essential to investigate the aerodynamic behavior associated with it. This paper emphasizes on study of the aerodynamic behaviors of the air flow around the train and tunnel when a train is located at different position relative to tunnel. Simulations of several position of the train with respect to the tunnel has been performed. The effect of Reynolds number, blockage ratio, several locations of train relative to tunnel, the number of bogies on the coefficient of drag (C_D) has been investigated. The effect of positions of the train relative to the tunnel on coefficient of pressure (C_P) has also been investigated. The processes involve the utilization of computational fluid dynamics (CFD) by using commercial software ANSYS Fluent. From the investigations, it is observed that the aerodynamic changes are more significant when train passes its tunnel entrance that are shown in velocity and pressure contour in Fig. 6 & 7; the train undergoes the maximum value of drag co-efficient (C_D) which is around 2.24. The vortex generated at the rear end of the train and between two bogies of the train are responsible for generating induced drag and induced moment on the train body that are shown in Fig. 8. These factors are related to the stability of a particular bogie of the train. The co-efficient of drag (C_D) increases with increasing the number of bogies, blockage ratio and decreases with increasing its Reynolds number. The changes of co-efficient of pressure (C_P) also shows a significant change for different locations that are related to the lift and moment on the train bogie.

Keywords: Train, Tunneling, Simulation, Incompressible, Boundary Layer

1. Introduction

Trains are essential vehicle for road transportation. It may affect largely on development of a country. It is very important facilities for regional economic and urban development. For the rapid development of train technology, many concerns have been given in various section about this technology. Noise reduction, passenger comfort, pressure wave concerns, effectiveness of velocity of the train, design geometry of the train etc. are the main concerns about this technology. For noise reduction, the tunneling and underground technology has become more popular day by day. But this technology has added more complexity [1].

Fig.1 Train entering tunnel [2]

When a train passing through a tunnel, the aerodynamic behavior has become more significant because, it is directly related to the driver and passengers' comfort. The fluctuation of air pressure, aerodynamic resistance, generation of complex patterns of air flow are the main problems in tunnel. These problems also fluctuate with the velocity of the train. This may lead to more complex condition in the train through tunnel. The idea of tunneling and underground train technology changes the concept of the aerodynamic effects which has become a big issue for train manufacturer. When a train moves in an open space, there generates a highly turbulent flow of air around the train. The turbulent flow region is called slipstream [3]. In this region, there causes significant aerodynamic changes. These changes can affect many problems for passengers on platform, driver and workers in tracksides. The stability of the train in different velocity condition may also be affected. In the high velocity of the train, there needs much stability and balancing of the train because, the train experiences a significant aerodynamic drag force and pressure as well as generates a larger pressure difference between inside and outside of the train.

When a train passes through a tunnel, the ability to flow of the air to dislocate to the side of the vehicle is decreased. For this reason, maximum air can flow to the front of the train and the ability to the flow of air in the rare position of the train is reduced. As a result, there generates a highly reduced pressure region in the rare side of the train which sucks air from the adjacent air region creates a flow in the side of the train and a high-pressure region in the front of the train. This phenomenon is called "piston effect" [4].

2. Methodology

2.1 Computational Domain and Boundary Conditions

There are five locations of the train with respect to tunnel. A computational domain with boundary conditions is shown in Fig. 2. The locations are given below:

* Corresponding author. Tel.: +88-01762089593
E-mail addresses: koushikahmed.me@gmail.com

•The train moving in an open environment
•The train approaching the tunnel entrance
•The train entering the tunnel
•The train entering about half of the train length
•The train passing through tunnel

The position of the train will be changed statically relative to tunnel. The geometries are created in model scaling which provides useful results that expresses flow behaviors that will exist in full scale environment. The dimensionless parameters will be same for both cases. The dimensions of train, tunnel and domain with blockage ratio 0.242 are given in Table 1.

Table 1 Dimensions of domain

Object	Parameters	Full size	1/50th
Domain	Length	271.8 m	5.536 m
	Height	48.375 m	0.9675 m
Train	Length	18.759 m	0.37518 m
	Height	2.7 m	0.054 m
Tunnel	Length	150 m	3 m
	Height	11.157 m	0.22314 m
	Thickness	1 m	0.02 m

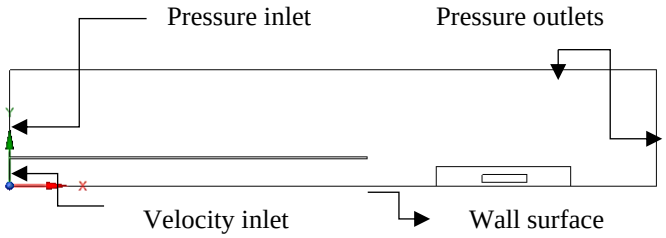

Fig. 2 Computational domain and Boundaries

The computational domain consists of five boundaries that are shown in Fig. 2. They are two different types of inlets (one pressure inlet and one velocity inlet), two outlets and one wall surface. The surface of the train is assumed no slip wall. The boundary conditions are shown in Table 2.

Table 2 Boundary Conditions

Boundary Section	Boundary Type	Value
Inlet 1	Pressure-inlet	0 Pa
Inlet 2	Velocity inlet	2.78 m/s
Top outlet	Pressure-outlet	0 Pa
Right outlet	Pressure-outlet	0 Pa
Bottom wall	Wall	No slip

2.2 Grid Generation and near wall treatment

An unstructured triangular patch conforming mesh was created using ANSYS meshing that is shown Fig. 3. Finer mesh was generated carefully near the train wall to capture boundary layer region. The average skewness was 0.11 and the orthogonal quality was 0.93.

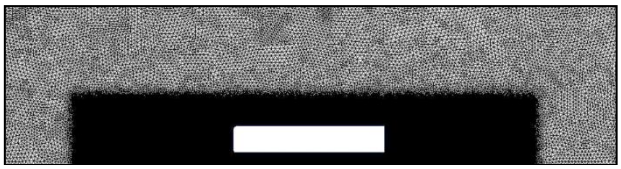

Fig. 3 Unstructured computational mesh

2.3 Governing equations

The governing equations to solve this numerical simulation are given below:

Continuity equation:

This equation takes the form:

$$\frac{\partial(\rho u_i)}{\partial x_i} = 0 \quad (1)$$

where ρ, t, u are the density, time and velocity components in the i direction, respectively.

Momentum equation

These equations take the following tensor form:

$$\frac{\partial(u_j \rho u_i)}{\partial x_j} + \frac{\partial p}{\partial x_i} - \frac{\partial \tau_{ij}}{\partial x_j} = 0 \quad (2)$$

The flow around the train is in a highly turbulent state.

The Reynolds number is calculated by formula:

$$Re = \frac{\rho V H}{\mu} \quad (3)$$

where the standard air density, ρ = 1.225 kg/m^3, V= Train Velocity, μ = Viscosity of air, H= Height of the train

In a turbulent steady flow, the flow variables fluctuate randomly in space. For this reason, statistical approaches can be used to define the flow. The flow variables can be decomposed into mean and fluctuating components, which is the basis of the Reynolds decomposition, Flow variables in the present work can be expressed as:

$u = \bar{u} + u'$

$p = \bar{p} + p'$

Now, the Reynolds decomposition is applied into the governing equations to obtain that is called the Reynolds Averaged Navier Stokes (RANS) equations. These equations take the form:

$$\frac{\partial(\rho \bar{u}_i)}{\partial x_i} = 0 \quad (4)$$

$$\rho \bar{u}_j \frac{\partial \bar{u}_i}{\partial x_j} = -\frac{\partial \bar{p}}{\partial x_i} + \frac{\partial}{\partial x_j}\left(\rho \nu \frac{\partial \bar{u}_i}{\partial x_j} - \rho \overline{u_i' u_j'}\right) \quad (5)$$

The subscripts i, j = 1, 2, 3 represent the x, y, z directions, respectively. The Reynolds stress tensor, which is $-\rho \overline{u_i' u_j'}$.

In order to close the RANS equations, an approximation for the eddy viscosity of the turbulent model is as follows:

$$-\rho\overline{u_i'u_j'} = \mu_t\left(\frac{\partial u_i}{\partial x_j}+\frac{\partial u_j}{\partial x_i}\right)-\frac{2}{3}(\rho k)\delta_{ij} \qquad (6)$$

where μ_t is the turbulent viscosity, which can be computed by the turbulent kinetic energy k and energy dissipation rate ε. Δ_{ij} is the Kronecker delta, while i= j, δ_{ij} = 1, while I ≠ j, δ_{ij} = 0.

$$\mu_t = \rho C_\mu \frac{k^2}{\varepsilon} \qquad (7)$$

where C_μ = 0.0845, and the transport equations of κ and ε are as follows:

$$\frac{\partial(\rho k u_i)}{\partial x_i} = \frac{\partial}{\partial x_i}\left[\alpha_k \mu_{eff}\frac{\partial \kappa}{\partial x_j}\right] + G_k + \rho\varepsilon \qquad (8)$$

$$\frac{\partial(\rho \varepsilon u_i)}{\partial x_i} = \frac{\partial}{\partial x_j}\left[\alpha_\varepsilon \mu_{eff}\frac{\partial \varepsilon}{\partial x_j}\right] + \frac{C_{1\varepsilon}^*}{k}G_k - C_{2\varepsilon}\rho\frac{\varepsilon^2}{k} \qquad (9)$$

2.4 Computational settings:

To solve these numerical simulations, the following set up, shown in Table 3, was Used.

Table 3 Solver settings for numerical analysis

Items	Inputs
CFD Simulation	2-D Double precision
Time	Steady
Solver	Pressure Based
Modeling	Turbulence
Turbulence Model	k-ε (2 equation)
k-ε Model	RNG
Near wall treatment	Standard wall function
Material type	Air
Pressure-velocity coupling	Coupled
Solution algorithm	Green-Gauge cell based
Turbulent Intensity	5%
Turbulent Viscosity	10%

3. Model Validation

A series of simulations were performed for mesh independence test. Mesh with different numbers of elements and nodes was generated. The variation of C_D with respect to number of elements are shown in Fig. 4. The test was performed for Reynolds number 500000 and blockage ratio 0.242. It was observed that meshes with number of elements higher than 514305 produced accurate result with minimum deviation. The number of elements less than 500000 causes a significant change in the value of C_D. Due to that mesh with element number 514305 was used for further simulations.

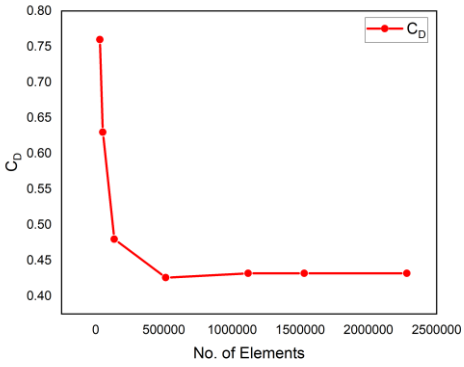

Fig. 4 Variation of C_D with no. of elements

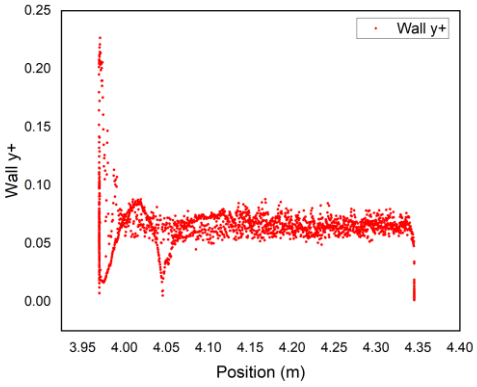

Fig. 5 Train wall Y+ vs position on train surface

A dimensionless wall parameter called y+ was kept less than 1. Fig. 5 shows the value of Y+ along the train surface. The boundary layer on the train wall surface can be captured accurately for this value. However, if enhanced wall treatment is used instead of standard wall treatment, the boundary layer region can be captured more accurately.

The results of this study have been validated by the experimental work of Aboutalebi, 2013 [5], [6] that are shown in Table 4 for three locations of the train. The blockage ratio of 0.242 and train speed of 2.78 m/s have been considered.

Table 4 Validation with Aboutalebi's study

Position of the train relative to the tunnel	C_D [5-6]	C_D (Present Work)	% Error
The train passing in an open space	0.436	0.43	1.3%
The train entering the tunnel	2.2	2.2383	1.74%
The train passing through the tunnel	1.15	1.25	8.6%

4. Results and Discussion

4.1 Contours

The characteristics of the aerodynamic behavior parameters such as pressure and velocity around the train body will be investigated in the symmetric surface of the computational domain.

The Fig.6 shows the complex airflow patterns around the train body by velocity contour plots. The velocity distribution around the train is significantly different for the different position of train relative to tunnel. From Fig.6, it is observed that a region of low velocity that is generated due to flow separation at the tail of the train for all cases. At this region, circulation occurs which causes drag force on the train body. In this region, a point is generated at which the net velocity is zero. Initially, at instant of the starting of the train, this point is above or near to the train body. After some time and with increasing train speed, the point goes away from the end. The air flowing around the train passing through the boundary layer region gets unstable for shear force exerted by no-slip train wall. As a result, the flow tends to rotate towards the tail of the train. This phenomenon generates a vortex that is called point vortex that are shown in Fig. 6 and Fig. 8 (Lower). A part of drag force due to viscous shear is generated due to this point vortex. The maximum velocity occurs at the nose of the train. At the curvature of the train nose, maximum velocity is induced because of high velocity gradient. The result also shows a significant changes of flow patterns when the train enters into the tunnel. The magnitude of maximum velocity occurs when entering the train nose into the tunnel and the magnitude of maximus velocity is 8.833 ms-1. It causes for passing the air through a small cross section between train surface the tunnel wall. It is called channeling.

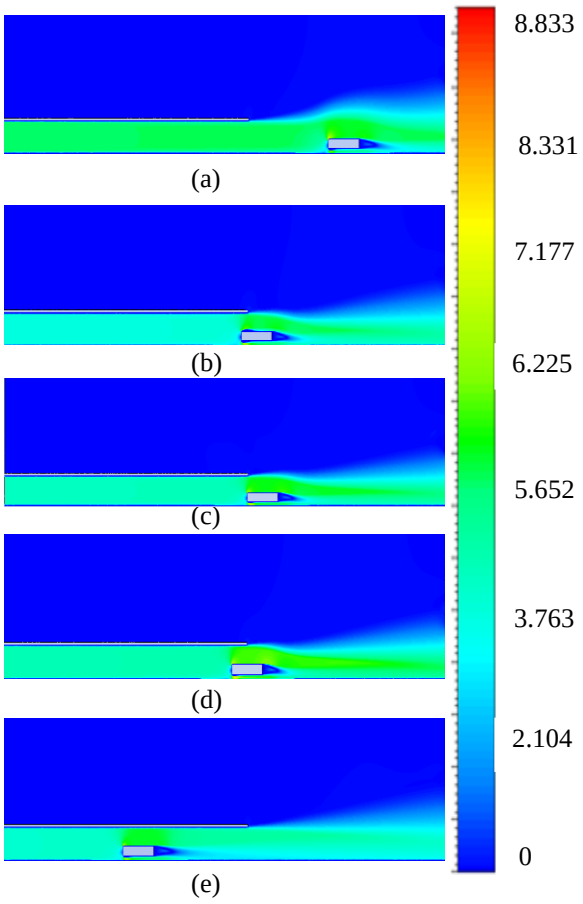

Fig. 6 Velocity Contours (m/s) for different train positions for Re=500000; (a) The train moving in an open environment (b) The train approaching the tunnel entrance (c) The train entering the tunnel (d) The train entering about half of the train length (e) The train passing through tunnel

The local pressure distribution around train body and the total domain are shown in Fig. 7.

It shows a large fluctuation of pressure distribution through the entire domain for the different position of bogie relative to the tunnel. The contours shows that a high-pressure region in the front of train nose and a low-pressure region that is called wake at the rear end of train tail. This is due to the fact that the air moving at the front of the nose gets resistance to flow at the rear end of the bogie. As a result, the air condensates at the front and it cannot easily flow to the rear end. So, a low-pressure region is generated at the rear end of the train bogie because of lack of air particles. This phenomenon is called piston effect. The first case shows a relatively stable pressure distribution through the entire domain when the train bogie runs at a constant speed in the open environment. But when the bogie approaches to enter into the tunnel the fluctuation of pressure distribution is much larger within a very small distance of the bogie. As the bogie moving towards the inside of the tunnel, the outside air tends to flow with the bogie towards the tunnel exit. For this reason, a low-pressure region is generated outside of the tunnel comparative to the tunnel inside.

This phenomenon occurs when the bogie is running near the tunnel entrance. When the train body is completely inside the tunnel, the aerodynamic local pressure distribution gets stable.

The vortex generated at the rear end of the train and between two bogies of the train are responsible for

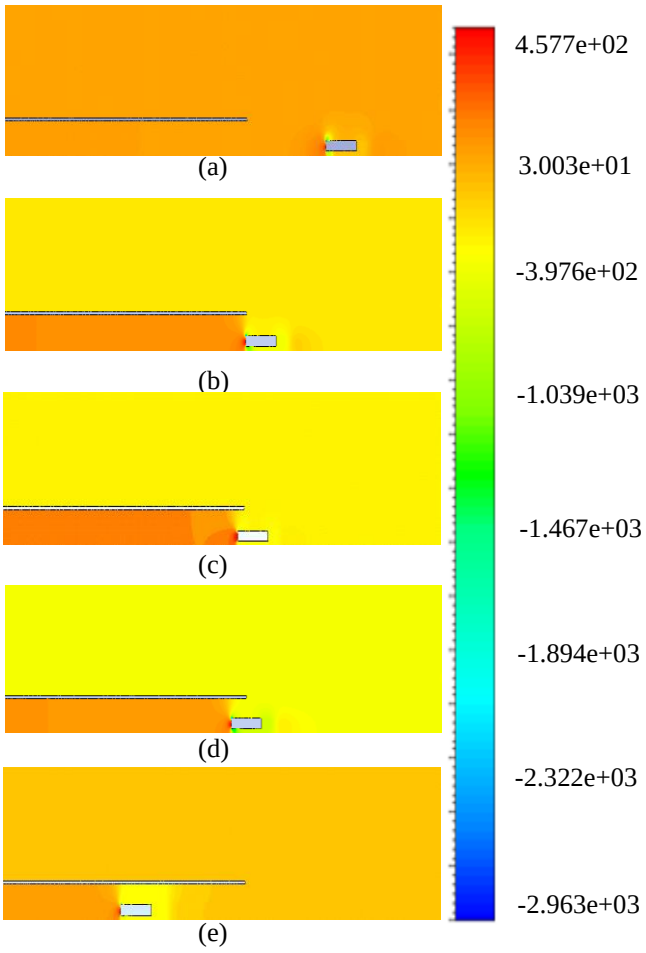

Fig. 7 Pressure Contours (Pa) for different train positions for Re=500000; (a) The train moving in an open environment (b) The train approaching the tunnel entrance (c) The train entering the tunnel (d) The train entering about half of the train length (e) The train passing through tunnel

generating induced drag and induced moment on the train body that are shown in Fig. 8. These factors are related to the stability of a particular bogie of the train.

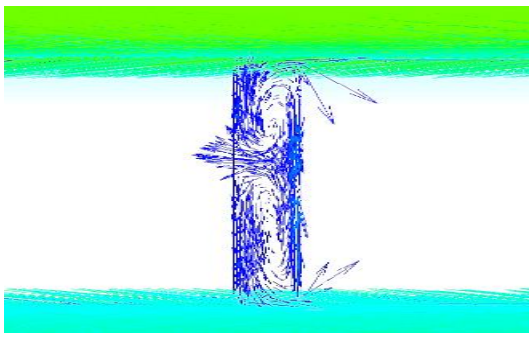

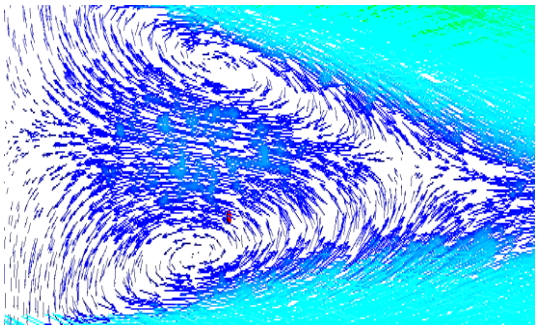

Fig. 8 Vortices generated between two bogies (Upper) and at the rare end of the train (Lower)

4.2 The effect of position of the train on drag co-efficient

Fig. 9 illustrates the behavior of drag the bogie has to face for two blockage ratios. The Reynolds number will be same for both cases. From the figure, it is seen that the value of the coefficient of drag is relatively small and stable when the train passes in an open space and its value is about 0.43. When a train passes through the tunnel entrance, the train faces a rapid pressure drag within a minimal distance, and the maximum value of the drag coefficient is around 2.24 for a blockage ratio of 0.242. After the train completes the entrance in the tunnel, the pressure drag gradually reduces and gets a quite stable value.

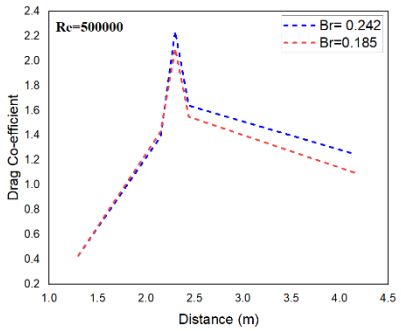

Fig. 9 Drag co-efficient vs train position of the train with one bogie

4.3 The effect of position of the train on Pressure co-efficient (C_P)

From Fig. 10, it is seen that when the train is moving in open space, the area under the curve of pressure co-efficient is less compared to the other two locations. So, the lift and moment generated on the bogie are less. When the train bogie entering the tunnel, it faces a significant drag as well as a large area under the curve, which denotes a large lift force. It is also seen that the train gets two opposite moments. For this reason, the train tends to rotate about Y-axis.

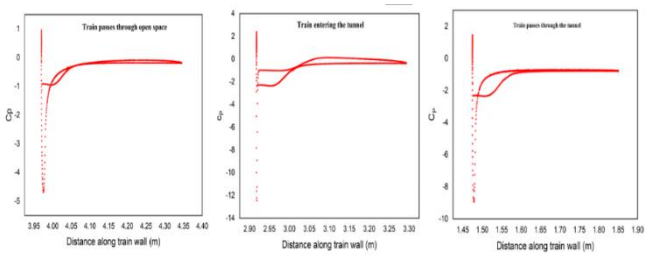

Fig.10 Pressure co-efficient on train wall for three locations of the train (train running open space: Left, Train entering tunnel: Middle, train running inside tunnel: Right)

4.4 The effect of Reynolds number on co-efficient of drag

Fig. 11 shows the different values of coefficient of drag on the different values of Reynolds number for two different locations of the train that are the train is moving inside the tunnel and outside the tunnel. This figure shows that the coefficient of drag decreases with the increase of the Reynolds number. If the Reynolds number increases, the boundary layer thickness around the train decreases as a thinner boundary layer. For this reason, the train wall undergoes a less viscous shear drag. As a result, the value of the drag coefficient decreases. So, the relation of the Reynolds number to the drag co-efficient is inversely proportional.

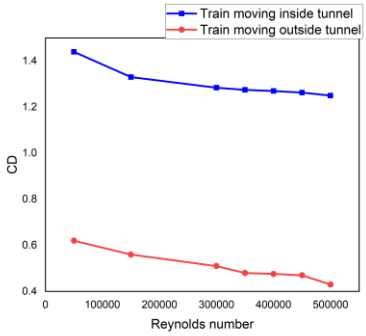

Fig. 11 Drag co-efficient vs Reynolds number

4.5 The effect of the number of bogies on drag co-efficient

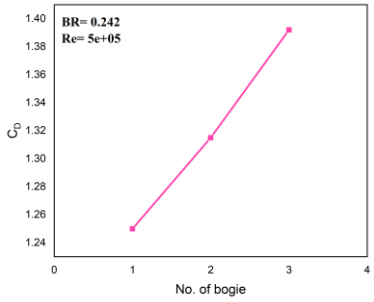

Fig.12 C_D vs number of bogies

From Fig. 12, shows a relationship between bogie number and coefficient of drag for a fixed Reynolds number and blockage ratio. It is seen that the train has to face more drag force as it has more bogies, and air passes through more walls of the train. So, the drag caused by the viscous effect increases with increasing the number of bogies.

4.6 The effect of blockage ratio on co-efficient of drag

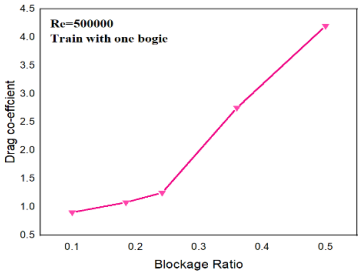

Fig. 13 Drag co-efficient vs blockage ratio

From Fig. 13, it is observed that the coefficient of drag increases significantly with increasing blockage ratio. This is due to the fact that the gap between train and tunnel becomes smaller with increasing the blockage ratio. As a result, the air to be passed by the train is harder than that of the smaller blockage ratio. This air gives a larger pressure force on the train body. This force contributes a larger drag force.

5. Conclusion

In this paper, aerodynamic characteristics of a train with one bogie have been studied using ANSYS Fluent by the Standard $\boldsymbol{k-\varepsilon}$ turbulence model. At the time of passing through tunnel entrance the aerodynamic changes occur more rapidly and significantly. So, the result will be more accurate if, a transient approach can be utilized. For this reason, the percentage error is more for this case. However, the result from the simulations using steady-state approach has provided a good appreciation with full-scale experiment.

6. References

[1] https://www.aar.org/wp-content
[2] https://www.Dreamstime.com
[3] Dong-Jin Zhu, 2017, "Aerodynamics of the metro train passing the tunnel with speed over 90 km/h", Journal of Vibro-engineering, Vol. 19, Issue 5, 2017, https://doi.org/10.21595/jve.2017.18427.
[4] Hui Yuan, Dan Zhou, Shuang Meng, 2019, 'Study of the unsteady aerodynamic performance of an inter-city train passing through a station in a tunnel'.
[5] Aboutalebi, H., 2013, "Experimental Study of Airflow Around a Train Entering a Tunnel" Master's Thesis, Department of Mechanical Engineering, Yazd University, Yazd.
[6] Rabani Mehrdad, Faghih K. ahmadreza, "Numerical analysis of airflow around a passenger train entering the tunnel", Journal of ELSEVIER, Tunneling and space technology (2015), 203-213

NOMENCLATURE

C_D : Co-efficient of Drag
Re : Reynolds Number
C_P : Co-efficient of Pressure